International Journal of Mechanical and Electrical Engineering
ISSN: 3005-9615 (Print), ISSN: 3005-7132 (Online) | Volume 6, Number 3, Year 2025
DOI: https://doi.org/10.62051/ijmee.v6n3.04
Journal homepage: https://wepub.org/index.php/IJMEE/index

Design and Testing of a Piezoelectric Ultrasonic Transducer

Zhenyu Liu

Tianjin University of Technology and Education, Tianjin, China

ABSTRACT

Carbon fiber composite materials have been widely used in the aerospace field. However, traditional milling processes struggle to meet their machining requirements. To achieve high-quality milling of carbon fiber composites, a compact sandwich transducer suitable for ultrasonic machining and capable of generating large amplitudes was proposed. Firstly, the basic dimensions of the stepped horn were designed based on wave propagation theory. Subsequently, a transducer model was established using Abaqus software, and modal analysis along with harmonic response analysis were conducted to verify the theoretical design. Finally, an experimental platform was built to perform impedance analysis and amplitude testing on the fabricated transducer. The results show that its maximum longitudinal output amplitude is 7.384μm. Its performance meets the requirements of most ultrasonic milling applications, thereby validating the correctness of the design methodology.

KEYWORDS

Ultrasonic Transducer; Simulation Analysis; Amplitude; Resonant Frequency.

1. INTRODUCTION

Carbon fiber reinforced polymer (CFRP) is widely used in the aerospace field, for applications such as aircraft fuselages, wings, and tails, and rocket structures including shells and wing surfaces. Traditional milling processes, when machining CFRP, are highly prone to rapid tool wear and induce defects in the CFRP workpieces such as burrs, delamination, and others [1]. Building upon conventional machining, researchers worldwide have iteratively upgraded the technique, leading to the proposal of ultrasonic vibration-assisted milling (UVAM). UVAM is achieved by superimposing periodic high-frequency vibrations onto the cutting tool during conventional milling. This technology offers significant benefits, including reduced milling forces, lower milling temperatures, and minimized defects in the finished CFRP parts, such as delamination, chipping, tearing, and burrs [2]. To match our self-developed ultrasonic generator and to enable better milling of finished CFRP products, an ultrasonic vibrator suitable for BT40 tool holders is proposed. This vibrator is designed to generate large vibration amplitudes while maintaining a compact length dimension.

The ultrasonic vibration system typically comprises an ultrasonic generator, a transducer, a horn, and the cutting tool. During the operation of the ultrasonic vibration system, the ultrasonic milling transducer serves as the core component within the ultrasonic milling system. Its performance and quality directly determine whether the ultrasonic vibration can be effectively transmitted to the cutting tool, consequently influencing the machining results [3]. Therefore, aiming to design an ultrasonic transducer, the structural parameters were designed and calculated based on wave propagation theory. Subsequently, modal analysis and harmonic response analysis were performed using Abaqus/CAE software to analyze the theoretically designed ultrasonic transducer. Finally, the designed transducer was fabricated and assembled. Vibration amplitude measurements was conducted to verify whether its performance meets the requirements of the ultrasonic machining system.

2. THEORETICAL DESIGN OF ULTRASONIC TRANSDUCER

Piezoelectric transducers exhibit superior characteristics such as high sensitivity, broad frequency response, high-temperature resistance, compact structure, and strong reliability. Based on these advantages, a piezoelectric transducer was selected for this system [4]. Its primary components include a front mass, piezoelectric ceramic rings, electrode shims, a rear mass, and a central bolt, collectively forming a sandwich-type cylindrical structure. The transducer was designed for an operating frequency of 22 kHz, a rated power of 800 W, and operates in the longitudinal vibration mode. To maximize machine tool travel and ensure overall coaxially, the ultrasonic vibrator employs a half-wavelength configuration. In this sandwich transducer design, the total length equals half the wavelength. Its vibrational characteristic is that the displacement amplitudes are maximum at both ends and are 180° out-of-phase, while a nodal plane (point of zero displacement) exists within the structure. By utilizing this nodal plane as the dividing interface, the entire transducer can be conceptually divided into two symmetrical quarter-wavelength resonators. A schematic diagram of the structure is illustrated in the Fig. 1.

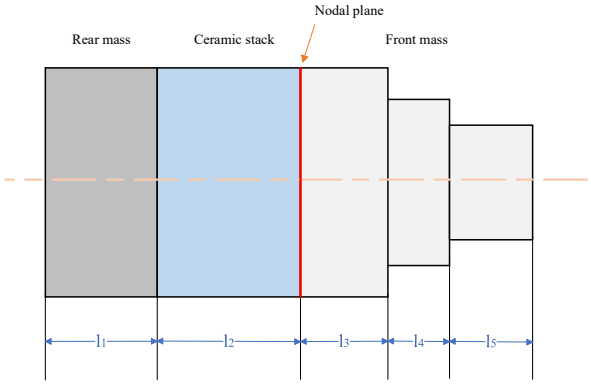

Figure 1. Schematic Diagram of Ultrasonic Vibrator

Regarding the selection of piezoelectric ceramic material, lead zirconate titanate (PZT-8) exhibits low field loss, a high electromechanical coupling coefficient, and strong piezoelectric constants. These properties enable it to meet the requirements for high-power operation and prolonged continuous duty cycles. Therefore, PZT-8 was selected as the piezoelectric ceramic material. Based on market availability, the thickness of a single piezoelectric ceramic disk was determined to be h=6mm. To prevent the generation of lateral vibrations, the diameter of the piezoelectric ceramic disks was constrained to be less than one-quarter of the operating wavelength. This constraint is expressed by the following relationship:

$$D \le \frac{\lambda_e}{4} \le \frac{C_e}{4f} = \frac{\sqrt{1/\rho_e s_{33}^d}}{4f}. \tag{1}$$

In Eq. (1), the diameter of the piezoelectric ceramic disk is denoted by D, and the wavelength within the piezoelectric ceramic material is denoted by λ_e. The designed resonant frequency is f=22 kHz, C_e represents the speed of sound in the material. Using the material density ρ_e=7.6×103kg/m^3 and the elastic compliance coefficient s_{33}^d=9.5×10-12m^2/N was calculated. Substituting these values into Eq. (1) yielded the result D≤50.85mm. Therefore, annular piezoelectric ceramic disks with an outer diameter of 50 mm and an inner diameter of 20 mm were selected for the transducer.

$$n = \frac{p_{max}}{p_e V_e f}. \tag{2}$$

In Eq. (2), Pmax denotes the maximum output power. To align with the operational requirements of the transducer, *P*max=800 W was selected. The parameter p_e represents the power capacity density of the piezoelectric ceramic material, assigned a value of 3W/kHz·cm^{-3}. The symbol V_e denotes the volume of a single piezoelectric ceramic disk.

The rear mass functions to enable unidirectional radiation of energy, thereby enhancing the output power at the front end of the transducer. To fulfil this functional requirement, the rear mass was fabricated from YG8 steel, a high-density material. The front mass ensures the efficient transfer of energy generated by the ultrasonic transducer along its longitudinal vibration direction. It requires low acoustic impedance and excellent fatigue resistance. Accordingly, the front mass was made from 45CrMo alloy steel, a material possessing high mechanical fatigue strength. The material parameters for each component of the transducer are listed in Table 1.

Table 1. Material Parameters of Transducer Components

Material	Elastic Modulus *E*(GPa)	Density *ρ*(kg/m3)	Wave Velocity *c*(m/s)	Wave number *k*	Wave length *λ*(mm)
42CrMo	206	7850	5122.7	4.29	146.4
YG8	400	14500	6350.6	4.6	123.7
PZT-8	123.0	7450	4063.3	5.41	116.1

For a slender rod with a non-uniform cross-section, composed of homogeneous and isotropic material, the wave equation for the rod can be derived under the following conditions: neglecting mechanical losses, assuming plane longitudinal waves propagate along the rod's axis, and assuming a uniform stress distribution across any transverse cross-section of the rod [5]. By substituting the boundary conditions into the wave equation derived from Newton's law, explicit design formulas for both the rear-mass and front-mass resonators are obtained, as shown in the Eqs. (3)-(4):

$$\tan(k_1 l_1)\tan(k_2 l_2) = Z_2 / Z_1 . \tag{3}$$

$$\frac{Z_5}{Z_4}\tan k_5 l_5 \tan k_4 l_4 + \frac{Z_5}{Z_3}\tan k_5 l_5 \tan k_3 l_3 + \frac{Z_4}{Z_3}\tan k_4 l_4 \tan k_3 l_3 = 1 . \tag{4}$$

The characteristic impedance is denoted by *Z*, and its expression is defined as:

$$Z = \rho_n c_n S(x_n) . \tag{5}$$

Based on the selected dimensions D1=D2=D3=50mm, D4=30mm, D5=14mm, the lengths of the rear mass and front mass were calculated. The resulting length dimensions are as follows: l1=11mm, l2=24mm, l3=7mm, l4=29mm, l5=24mm. These parameters will be used for subsequent modal analysis and harmonic response analysis to verify compliance with design requirements.

3. FEA OF ULTRASONIC TRANSDUCER

3.1. Modal Analysis

Modal analysis aims to identify the natural frequencies and corresponding mode shapes of the transducer. By analyzing dynamic characteristics at resonant frequencies, it ensures the transducer's safety, stability, and reliability in operation. The 3D model of the designed horn along with the ER collet and double-edge milling tool was assembled and imported into ANSYS for modal analysis with material properties assigned to each part. For meshing, hexahedral mesh was used for the rear mass and piezoelectric stack, while tetrahedral mesh was applied to other components, with a shared-node connection as the contact type and unconstrained boundary conditions. The frequency sweep

parameters were set as a range of 18–25 kHz with a step size of 50 Hz. The resonant mode characteristics indicate that the longitudinal mode occurs at 20.746 kHz with pure axial vibration. The Fig. 2 illustrates the deformation of the longitudinal mode. The actual resonant frequency is lower than the theoretical design value, attributed to the added mass of the ER collet and tool. This frequency shift is a normal occurrence and meets the design requirements.

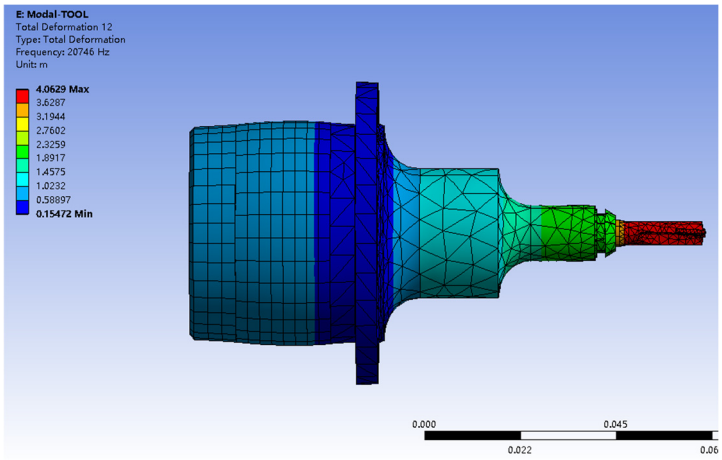

Figure 2. The Deformation of The Longitudinal Mode

3.2. Harmonic Response Analysis

The harmonic response analysis of the transducer calculates its dynamic response under periodic resonant excitation through numerical methods. This analysis can obtain key parameters such as the amplitude-frequency characteristics, resonant frequency, and vibration amplitude of the transducer [6]. The analysis frequency range was set to 20-22 kHz with 50 solution substeps, and a 6V high-frequency excitation voltage was applied to the piezoelectric ceramic stack. The amplitude-frequency response curve is shown in Fig.3(a), which indicates that the resonant frequency corresponding to the peak Z-direction displacement amplitude at the end face is 20.700 kHz. Additionally, when a 20.746 kHz high-frequency electrical excitation is applied to the transducer with the tool attached, the Z-direction amplitude of the tool can reach 4.9466μm, with the specific vibration amplitude results shown in the Fig. 3(b). The consistency between the harmonic response analysis results and the modal analysis results confirms the reliability of the design.

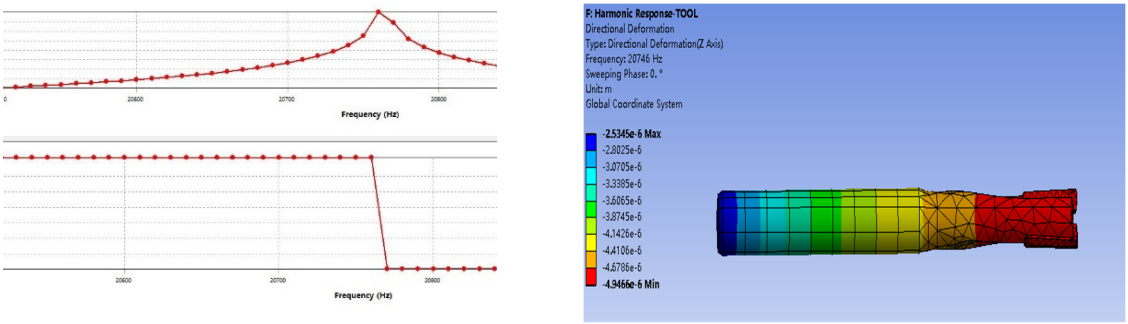

(a) (b)

Figure 3. The Harmonic Response Result of The Longitudinal Mode

4. EXPERIMENTAL TESTING OF ULTRASONIC TRANSDUCER

The transducer fabricated according to the designed dimensions is shown in Fig. 4. The ultrasonic horn machined mounting threads for securing the machining collet and cutting tool. To validate the dimensional accuracy and operational performance of the vibrator, further verification requires:

quantitative measurement of output end-face amplitude using a laser Doppler vibrometer during ultrasonic generator excitation.

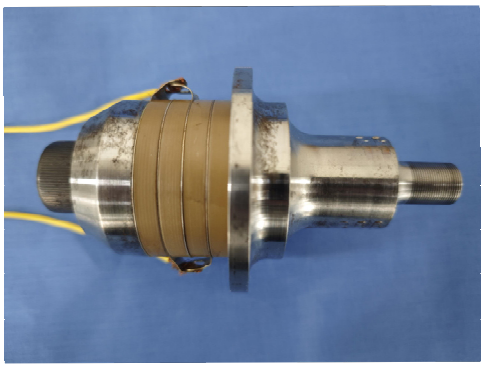

Figure 4. Fabricated Transducer

Considering machining tolerances may cause deviations between measured and theoretical amplitudes, this experiment conducted ultrasonic amplitude measurements with the vibrator installed on the machine tool. To ensure experimental compliance, an ultrasonic generator supplied electrical oscillation signals to the vibrator, achieving precise power control through coordinated adjustment of its internal calibration coefficient and external output percentage. Amplitude quantification was performed using a laser Doppler vibrometer, with the test configuration shown in Fig. 5.

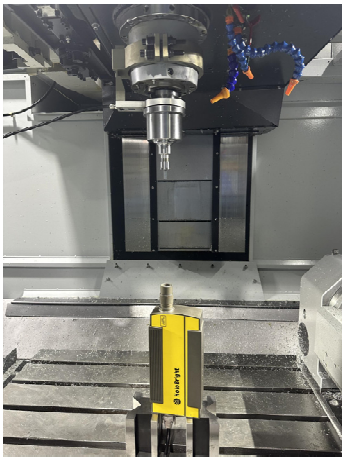

Figure 5. Test Configuration

The amplitude measurement results presented in the Table 2 demonstrate that as ultrasonic power increases, the output amplitude rises within a range of 0μm to 7.4μm micrometers. The deviation between actual vibration frequency and simulation/theoretical analysis remains controlled at approximately 5%. Based on these experimental data, it is confirmed that this ultrasonic vibration system satisfies the requirements for ultrasonic vibration-assisted milling experiments.

Table 2. Test Results of Vibration Amplitude

Group	Power (%)	Amplitude (μm)
1	10%	0.894
2	25%	1.832
3	40%	3.810
4	55%	4.759
5	70%	6.392
6	85%	7.384

5. SUMMARY

Based on the results and discussions presented above, the conclusions are obtained as below:

(1) Theoretical calculations determined the number of piezoelectric ceramic disks and component dimensions. Modal and harmonic response analyses in ANSYS validated the accuracy of these design parameters, confirming a maximum amplitude of 4.9466μm under 20.764kHz high-frequency excitation. The transducer was subsequently fabricated based on these results.

(2) Measurements of the tool amplitude under mounted machine tool conditions confirmed an adjustable range of 0μm to 7.4μm, thus confirming the transducer's compliance with CFRP ultrasonic vibration milling requirements.

REFERENCES

[1] Wang, C., Liu, G., An, Q. and Chen, M. (2017). Occurrence and formation mechanism of surface cavity defects during orthogonal milling of CFRP laminates. Composites Part B: Engineering, Vol. 109, pp. 10–22. https://doi.org/ 10. 1016/j.compositesb.2016.10.015.

[2] Khan, M.A., Ali, A.B.M., Ullah, S., et al. (2025). A review on recent advancements in ultrasonic vibration-assisted machining of difficult-to-machine materials. International Journal on Interactive Design and Manufacturing. https://doi.org/10.1007/s12008-025-02306-6.

[3] Zheng, L., Chen, W. and Huo, D. (2020). Review of vibration devices for vibration-assisted machining. The International Journal of Advanced Manufacturing Technology, Vol. 108(3), pp. 1631–1651. https://doi.org/ 10.1007/ s00170-020-05483-8.

[4] Zhou, H., Zhang, J., Yu, D., Feng, P., Wu, Z. and Cai, W. (2019). Advances in rotary ultrasonic machining system for hard and brittle materials. Advances in Mechanical Engineering, Vol. 11(12). https://doi.org/10. 1177/ 1687814019895929.

[5] Ahmad, S. (2024). Implementation of new stepped horn in rotary ultrasonic machining of NOMEX honeycomb composites. Journal of Mechanical Science and Technology, Vol. 38(12), pp. 4983–4988. https://doi.org/ 10. 1007/s12206-024-0834-1.

[6] Yang, L., Han, X., Xie, Y., Lv, Q. and Liu, E. (2025). Design and experimental study of catenary linear horn based on ultrasonic machining. Processes, Vol. 13(3), pp. 714. https://doi.org/10.3390/pr13030714.